Published in final edited form as:
Timing Time Percept. 2014 May 19; 2(2): 145–168. doi:10.1163/22134468-00002025.

Dissociation of Neural Mechanisms for Intersensory Timing Deficits in Parkinson's Disease

Deborah L. Harrington[1,2,*], **Gabriel N. Castillo**[1,2], **Jason D. Reed**[1,2], **David D. Song**[3,4], **Irene Litvan**[4], **Roland R. Lee**[2,5]

[1]Research Service, VA San Diego Healthcare System, San Diego, CA, USA

[2]Department of Radiology, University of California San Diego, La Jolla, CA, USA

[3]Neurology Service, VA San Diego Healthcare System, San Diego, CA, USA

[4]Department of Neuroscience, University of California San Diego, La Jolla, CA, USA

[5]Radiology Service, VA San Diego Healthcare System, San Diego, CA, USA

Abstract

This study investigated the ability of individuals with Parkinson's disease (PD) to synthesize temporal information across the senses, namely audition and vision. Auditory signals (A) are perceived as lasting longer than visual signals (V) when they are compared together, since attentsion is captured and sustained more easily than for visual information. We used the audiovisual illusion to probe for disturbances in brain networks that govern the resolution of time in two intersensory conditions that putatively differ in their attention demands. PD patients and controls judged the relative duration of successively presented pairs of unimodal (AA, VV) and crossmodal (VA, AV) signals whilst undergoing fMRI. There were four main findings. First, underestimation of time was exaggerated in PD when timing depended on controlled attention (AV), whereas subtle deficits were found when audition dominated and attention was more easily sustained (VA). Second, group differences in regional activation were observed only for the AV-unimodal comparison, where the PD group failed to modulate basal ganglia, anterior insula, and inferior cerebellum activity in accord with the timing condition. Third, the intersensory timing conditions were dissociated by patterns of abnormal functional connectivity. When intersensory timing emphasized controlled attention, patients showed weakened connectivity of the cortico-thalamus-basal ganglia (CTBG) circuit and the anterior insula with widespread cortical regions, yet enhanced cerebellar connectivity. When audition dominated intersensory timing, patients showed enhanced connectivity of CTBG elements, the anterior insula, and the cerebellum with the caudate tail and frontal cortex. Fourth, abnormal connectivity measures showed excellent sensitivity and specificity in accurately classifying subjects. The results demonstrate that intersensory timing deficits in PD were well characterized by context-dependent patterns of functional connectivity within a presumed core timing system (CTBG) and a ventral attention hub (anterior insula), and enhanced cerebellar connectivity irrespective of the hypothesized attention demands of timing.

[*]To whom correspondence should be addressed. dharrington@ucsd.edu.

Keywords

Interval timing; time perception; Parkinson's disease; audiovisual illusion; functional imaging

1. Introduction

Temporal processing disturbances in Parkinson's disease (PD) are of keen interest, owing to the centrality of the striatum and dopamine neurotransmission in explicit timing (Agostino et al., 2011; Balci et al., 2013; Coull et al., 2012; Lake & Meck, 2013; Matell & Meck, 2004; Meck, 1996). The clinical relevance of timing deficits in PD is further underscored by the benefits that external rhythmic-pacing cues confer on movement stability, accuracy, and fluency (Lee et al., 2012; Majsak et al., 1998; McIntosh et al., 1997; Nieuwboer et al., 2009; Spildooren et al., 2012; Vercruysse et al., 2012). However, timing dysfunction is not simply due to motor symptoms, since it is found when motor output is minimized (Artieda et al., 1992; Harrington et al., 1998, 2011b; Koch et al., 2004a, b; Malapani et al., 2002; Pastor et al., 1992; Rammsayer & Classen, 1997; Riesen & Schnider, 2001). Nevertheless, unraveling the neurocognitive bases of timing deficits in PD has proved challenging, since they could arise from changes in the presumed core striatal timing-mechanism (Matell & Meck, 2004), but perhaps also in interacting systems that are selectively engaged depending on the cognitive and sensorimotor requirements of a behavioral context (Merchant et al., 2013a). For example, timing-related dysfunction of the cortico-thalamic-basal ganglia (CTBG) circuit [i.e., striatum, supplementary motor area (SMA)] and the working memory system in PD patients was largely context-dependent, as was the effect of dopamine therapy on brain functioning (Harrington et al., 2011b). Though intriguing, the neural mechanisms of time perception deficits in PD are not well understood, owing to the dearth of functional imaging studies and the focus on simple forms of timing within the same modality.

The present study sought to address this knowledge gap by investigating the ability of PD participants to synthesize temporal information across a common pairing of the senses, namely audition and vision. In naturalistic settings, we routinely combine temporal information from different senses into a single perceptual experience. This is of relevance to PD since the striatum is involved in multisensory integration (Nagy et al., 2006) and governs intersensory timing (Dirnberger et al., 2012; Harrington et al., 2011a). An important feature of intersensory timing is that its resolution depends on the signal modalities, such that auditory signals (A) are perceived as lasting longer than visual signals (V) of the same physical duration when they are compared together. As such, time is dilated when the duration of an auditory comparison interval is judged relative to a visual standard interval (VA) and compressed when a visual comparison interval is judged relative to an auditory standard (AV) (Harrington et al., 2011a; Ulrich et al., 2006; Wearden et al., 1998). The audiovisual 'illusion' is related to the dominance of audition over vision in the context of timing (Chen & Yeh, 2009; Klink et al., 2011; Mayer et al., 2009; Merchant et al., 2008b; Repp & Penel, 2002). Models such as Scalar Expectancy Theory (SET) (Gibbon et al., 1984) attribute the illusion to a pacemaker-accumulator system that runs faster for A than V signals, owing to the shorter interpulse time, and/or an attention switch that permits a faster accumulation of pulses for auditory signals (Lustig & Meck, 2011; Penney et al., 2000;

Ulrich et al., 2006; Wearden et al., 1998). Thus, auditory signals appear to capture and sustain attention more automatically than visual signals (Berry et al., 2014). Audiovisual timing is normally mediated by thestriatum, and cognitive-control systems(SMA and pre SMA, middle an dinferior frontal gyrus) exhibit greater activation when time is compressed (AV) than when it was dilated (VA) (Harrington et al., 2011a). The latter finding is compatible with the greater attentional demands of timing visual signals, which if not sustained, leads to a loss in pulses.

The present study used the audiovisual illusion to identify the neural mechanisms of expected intersensory timing deficits in PD and to determine if they were governed by the presumed attention demands of timing visual and auditory signals. Healthy controls and PD patients judged the relative duration of pairs of unimodal (AA, VV) and crossmodal (VA, AV) signals. Unimodal timing of auditory and visual signals results in more accurate percepts than multisensory timing (Harrington et al., 2011a; Ulrich et al., 2006), which activates larger sets of cortical structures that are thought to serve as the clock signal (Matell & Meck, 2004) and hence, may place greater demands on detection and integration of cortical oscillatory time-codes by the striatal timing-system. Indeed, we reported stronger striatal interactions with the cortex for multisensory than unimodal timing, but also stronger cortico-cortical interactions among networks that support attention and executive-control (Harrington et al., 2011a). As such, we predicted that timing deficits in PD patients would be greater in both of the crossmodal conditions relative to the unimodal conditions, largely owing to problems adjusting striatal activity in accord with the increased demands of multisensory timing. If cognitive-control disturbances also contribute to impaired intersensory timing (Harrington et al., 2011b), we predicted that PD patients would show greater deficits in the AV condition, owing to the hypothesized increased attentional control required for timing visual signals (Berry et al., 2014; Lustig & Meck, 2011), and that this result would be associated with abnormal functioning of executive and/or attention networks. To explore these hypotheses further, we compared the groups to determine if the effective connectivity of the CTBG circuit and other key timing-related regions was weakened or strengthened in the PD group for each of the crossmodal conditions in comparison to unimodal timing. Lastly, cortical and subcortical volumes were assessed to determine if the functionality of brain systems in PD partly depends on the structural integrity of grey-matter tissue.

2. Materials and Methods

2.1. Participants

Study participants consisted of 27 patients with a diagnosis of idiopathic PD and 24 healthy controls. Procedures were approved by the University of California, San Diego (UCSD) Human Research Protections Program. The study was performed in accordance with ethical guidelines in the 1964 Declaration of Helsinki. All subjects provided written informed consent. Subjects were excluded from participation if they had metal in their head, neurological diagnoses other than PD, psychiatric diagnoses, history of alcohol or substance abuse, and cognitive impairment as defined by a score of less than 26 on the Mini Mental Status Exam (MMSE). PD patients met the PD United Kingdom Brain Bank Criteria. The

groups did not differ in gender composition, years of education, age, or MMSE scores (Table 1). Patients had a PD diagnosis for an average of 5.6 (SD = 4.6) years. Four patients were taking levodopa/carbidopa monotherapy, two were on rasagiline monotherapy, and 21 were on levodopa/carbidopa and DA agonists. The mean levodopa equivalence (LED) was 706.10 (SD = 431.06) (Razmy et al., 2004). Motor symptoms were assessed when patients were 'on' and 'off' dopamine therapy using Part III of the Unified Parkinson's Disease Rating Scale (UPDRS) and the Hoehn and Yahr scale. As expected, symptoms on the UPDRS were worse off [mean = 33.4 (SD = 11.0)] than on [mean = 25.4 (9.7)] medications [$t_{26} = -6.07$, $p < 0.001$]. On the Hoehn and Yahr scale, 60% of the patients had a stage 2, both on and off medication; the remaining had a stage 3. To better characterize cognitive functioning of the PD sample, a battery of neuropsychological tests was administered to PD participants while on medication and to controls. The groups did not differ on measures of executive functioning, visual cognition, or memory (Table 1), except for slightly poorer Letter Fluency performance in the PD group. The night before the fMRI session, PD participants refrained from taking medication for about 2 half-lives of the longest acting medication (about 14 to 16 h before the scan), so that they underwent fMRI scanning in a 'practical' off state.

2.2. Time Discrimination Task

Participants performed a time perception task similar to that described by Harrington and colleagues (Harrington et al., 2011a) while undergoing fMRI. The task design is illustrated in Fig. 1. Subjects attended to the duration of successively presented pairs of auditory (A; 1000 Hz pure tones) and visual (V; blue ellipse) stimuli, and judged whether the second stimulus (comparison interval; CI) was shorter or longer than the first stimulus (standard interval; SI) by respectively pressing a key with the right index or middle finger. Tone stimuli were delivered binaurally through a headphone that together with earplugs attenuated background scanner noise by about 40 db. Visual stimuli were viewed through a NordicNeuroLab goggle system. In the unimodal conditions the SI and CI were the same modality (AA, VV) and in the crossmodal conditions they were different (AV, VA). Throughout the experiment, the subject fixated on a white cross at the center of the display. Prior to trial onset, a warning signal (flashing yellow cross and mixed 700 Hz tone) appeared for 350 ms followed by a 500 ms delay. The trial began with the presentation of the SI, followed by a variable delay (1200 to 1500 ms), and then the CI. Four SIs were used to increase trial-by-trial interval encoding demands (Fig. 1, bottom). For each SI, there were three shorter and longer CIs that differed from the SI duration by increments of ±7%. Accuracy and reaction time (RT) were recorded. The analyses averaged across the SI durations and the CI durations that were ±7, 14, and 21% increments of the SI.

For each condition (AA, VV, AV, VA), there were 24 trials and four trials per CI. The order of conditions was randomized across four runs, each lasting 6 min 20 s. At the end of the CI, there was a 3 s window for subjects to make their response. The inter-trial jitter of 4021 to 9200 ms allowed for the best sampling of the hemodynamic response and establishment of a baseline resting state (i.e., fixation plus ambient scanner noise). Six filler images were added to the beginning and end of each run to respectively allow for T1 equilibration and the delayed hemodynamic response of the final trial. Before imaging, subjects practiced a version of the task that used different SI durations (950 and 1100 ms).

2.3. MRI Acquisition

Event-related fMRI was conducted at the UCSD Center for FMRI on a GE 3-T Excite MRI system equipped with an eight-channel head coil. Foam padding was used to limit head motion in the coil. Echo-planar images (EPI) were acquired using a single-shot, blipped, gradient-echo, echo-planar pulse sequence (TE 30 ms, TR 2.0 s, 90° flip angle, FOV 24 cm, 64 × 64 matrix, NEX 1, interleaved slice acquisition). Each functional imaging volume included 37 contiguous, axial 4 mm slices (3.75 mm × 3.75 mm × 4 mm voxel size) that provided coverage of the entire brain. High-resolution T1-weighted anatomic images were collected for registration with the EPI (TE 3.0 ms, TR 7.8 ms, 12° flip angle, NEX 1, 1-mm axial slice thickness, FOV 25 cm, 256 × 256 matrix) and for analyses of gray-matter volume.

2.4. fMRI Analysis

Data were processed using Analysis of Functional Neuroimaging (AFNI) software (Cox, 1996). The first four pre-steady-state volumes of the EPI time series were removed. The remaining images were slice-time corrected, motion corrected, and spatially smoothed using a 8 mm FWHM Gaussian filter. For each participant, the time series was deconvolved using SI onset for the four trial types: AA, VV, AV, and VA. The deconvolution modeled 8 TRs (16 s). Six demeaned head-motion parameters were included as covariates of no interest. Area under the curve (AUC) was calculated using 8 s of activation beginning at 6 s post-trial onset, to capture the peak activation throughout the trial. Time points with more than 0.3 mm deviation in any one direction were censored from the dataset. AUC maps were then interpolated to 4 mm isometric voxels, co-registered, and converted to Talairach coordinate space.

In the first level of analysis, paired *t*-tests were performed on a voxelwise basis separately for each group to generate statistical parametric maps that identified voxels for two contrasts of interest, namely (1) unimodal (AA, VV)–AV and (2) unimodal–VA. Voxelwise statistical thresholds were derived from 5000 Monte Carlo simulations (3dClustSim) that computed the voxel probability and minimum cluster size threshold needed to obtain a 0.05 familywise alpha. Because spatial thresholds are biased against smaller activation clusters of a priori interest, thresholds were derived separately for basal ganglia (caudate, putamen, globus pallidus) and cortical (all other brain regions) volumes. The familywise alpha (0.05) was obtained using a voxelwise probability of $p = 0.004$ and a minimum cluster size of 1.088 ml for the cortex and a voxelwise probability of $p = 0.009$ and a minimum cluster size of 0.512 ml for the basal ganglia. At a second level of analysis, a disjunction mask was created for each contrast by combining all suprathreshold voxels from each of the group *t*-maps. This produced functional ROI (fROI) maps for each of the two subtraction conditions. Then mixed model repeated-measure ANOVAs were applied to the AUC to test the group and the group × timing condition interaction effects for each fROI and contrast condition. The false discovery rate (FDR) was used to correct for multiple group comparisons.

2.5. Effective Connectivity Analyses

The psychophysiological interaction (PPI) method (Friston et al., 1997) was used to determine if the connectivity strength of a region of interest (ROI) or ‘seed’ was modulated by the timing condition (i.e., experimental variable) differently for the PD and control

groups. The CTBG network seeds included the (1) left and right caudate head, (2) left and right caudate body, (3) left and right putamen, (4) left and right globus pallidus (GP), (5) bilateral SMA, and (6) bilateral preSMA. Other seeds included the (1) right anterior insula and (2) the left semi-lunar lobule, the selection of which was driven by the results from the conventional fROI analyses. All seeds were constructed from timing-related activation in the fROI regional analyses. The basic processing steps in the PPI analysis included: (1) bandpass filtering (0.001 to 0.1 Hz) of individual raw EPI signal; (2) white-matter masks were generated for each subject (FSL's fast anatomical segmentation) and used to extract the WM signal; (3) individual time courses in the processed dataset were extracted for each seed region; and (4) seed time courses were detrended and deconvolved using a gamma function to remove hemodynamic delay. The resultant seed-region signal was multiplied by a condition of interest regressor, thereby creating an interaction time course, which was convolved with a gamma-variate HRF (AFNI waver). The first regressor (physiological variable) represented the time series of activity from the seed ROI. The second regressor (psychological variable) represented the timing condition (e.g., 1 for unimodal and −1 for crossmodal) and used a 4 s boxcar function. The PPI regressor was computed as the cross-product of the physiological variable and the psychological variable. The regression model included nuisance (baseline differences, linear drift, head movement, fluctuations in white-matter signal), the seed time-course, task regressors, and the PPI regressor. The PPI regressor produces correlation maps of a seed time-course with the time course from all other brain voxels as a function of the psychological variable (e.g., unimodal versus crossmodal). Correlation maps were transformed to Fisher Z scores. A second level of analysis conducted group comparisons (independent t-tests) on the strength of connectivity (Fisher Z) of the seed region with other brain voxels using a voxelwise probability of $p = 0.004$ and minimum cluster size 0.512 ml (uncorrected for multiple comparisons). Group comparisons were then FDR corrected separately for the VA and AV PPI analyses to adjust for multiple comparisons. Since connectivity is typically stronger for crossmodal than unimodal timing in young adults (Harrington et al., 2011a), only PPI tests demonstrating stronger connectivity for the AV or VA conditions relative to the unimodal condition in one or both groups were reported due to the focus of the present study on crossmodal timing.

2.6. Structural MRI Analysis

Anatomical scans were analyzed using a parcellation method in FreeSurfer 5.1 software (Fischl et al., 2004) to evaluate group differences in brain atrophy. This automated approach provides anatomically accurate renderings of regional volumes without potential rater bias (Fischl et al., 2001). Volumes of the frontal, parietal, temporal, and occipital lobes, the cerebellum, and subcortical structures (caudate, putamen, globus pallidus, thalamus) were compared between the two groups, separately for each hemisphere. Total cerebral spinal fluid volume (CSF) was also examined. Volumes were divided by estimated total intracranial volume (eTIV) to adjust for differences in head size.

3. Results

3.1. Time Perception Performance

Accuracy data were converted to the percent longer responses for each CI that was ±7, 14, and 21% shorter/longer than the SI. A mixed-model ANOVA tested the effects of group, timing condition (unimodal, crossmodal), CI modality, CI duration, and the interactions. The group × timing condition × CI duration interaction (F (1, 49) = 4.93, p = 0.03) showed a progressive underestimation of time in the PD group relative to controls as the CI duration increased (Fig. 2A), but only in the two crossmodal conditions (group × CI duration: F (1, 49) = 9.16, p = 0.004 for VA condition; F (1, 49) = 5.77, p = 0.02 for AV condition). Group × CI duration interactions were not found for unimodal auditory or visual signals. Thus, in both crossmodal conditions, PD patients progressively underestimated time as the CI duration increased, consistent with a slowing of the hypothetical timekeeper. In addition, the group × timing condition × CI modality interaction (F (1, 49) = 5.24, p = 0.026) showed that relative to the two unimodal conditions (AA, VV) the PD group underestimated the duration of AV pairs more than the control group (p = 0.006) (Fig. 2B). Time compression was therefore exaggerated in the PD group. No other group effects were found for accuracy, nor did the groups differ in RT. In both groups, RTs were longer for crossmodal (824 ms) than unimodal (788 ms) pairs (F (1, 49) = 6.32, p 0.015), owing to longer RTs for AV (873 ms), but not VA (775 ms) pairs (timing condition × CI modality: F (1, 39) 15.71, p = 0.0001). This finding suggests that in both groups, AV decisions were more difficult than for the other stimulus pairs.

3.2. fROI Analyses

Figure 3A and Tables 2 and 3 display the results from the disjunction analysis, which identified 13 fROI for the unimodal–AV subtraction and 8 fROI from the unimodal–VA subtraction. For both subtractions, differences in activation were observed between the unimodal and each crossmodal condition for the bilateral SMA, right inferior frontal gyrus, bilateral superior temporal gyrus, and various visual centers of the occipital-temporal cortex. Notable exceptions included the basal ganglia, the right anterior insula, and the left inferior cerebellum, which showed timing-condition effects only for the unimodal–AV subtraction.

For the unimodal–AV comparison (Fig. 3A, left column; Table 2), activation was greater for the AV than the unimodal timing condition in a large cluster consisting of the bilateral cuneus, left precuneus, and left angular gyrus, the right precuneus, and the right middle temporal gyrus. The remaining fROI showed greater activation for the unimodal than the AV condition in the bilateral SMA/cingulate, left precentral/postcentral gyrus, right inferior frontal gyrus, right anterior insula, bilateral superior temporal gyrus, the bilateral caudate, putamen, and globus pallidus, and the left inferior semi-lunar lobule. Significant group × timing condition interactions (FDR corrected) were found for five of these fROI, which are marked by superscript numbers in Table 2, and displayed and graphed in Fig. 3B and C. Figure 3C shows that in the control group, MR signal intensity was significantly greater for unimodal than the AV timing condition (p <0.001) for all three basal ganglia fROI, the right anterior insula, and the left cerebellum (inferior semi-lunar lobule). In the PD group, activation did not differ significantly between the timing conditions for these fROI except

for the left caudate head, which showed greater MR signal intensity for the AV than the unimodal condition ($p = 0.02$). No other group effects were significant. These results demonstrate prominent deficits in PD patients in the ability to modulate striatal, insula, and cerebellar activity when the intersensory synthesis of time was putatively more attention demanding.

For the unimodal–VA comparison (Fig. 3A, right column; Table 3), activation was greater for the VA than the unimodal timing condition in the bilateral superior temporal gyri. The remaining fROI showed greater activation for the unimodal than the VA condition, including the right preSMA/cingulate, bilateral SMA/cingulate, right IFG, the right parahippocampus, and a large cluster consisting of the bilateral middle occipital cortex, lingual and fusiform gyri and the occipitotemporal cortex. Of these regions, no group differences or group interactions with timing condition were significant for the unimodal–VA comparisons (FDR corrected). These findings suggest that PD patients were able to modulate cortical activities in a normal manner when the intersensory synthesis of time presumably was less attention demanding.

3.3. Effective Connectivity Analyses

We then examined whether AV and VA timing deficits in the PD group were related to altered connectivity of the seed fROIs. Tables 4 and 5 summarize the results from the PPI analyses that contrasted functional connectivity for the unimodal condition with each crossmodal condition and tested for group differences. All group independent *t*-tests were significant after FDR correction of multiple comparisons. The network connectivity maps of these results are shown in Fig. 4.

In the control group (Table 4; Fig. 4A), connectivity of the CTBG circuit and the right anterior insula was stronger for AV than for unimodal timing. Connectivity of these seeds was enhanced with frontal, temporal, and parietal areas. This included stronger AV connectivity of: (1) the bilateral caudate head and body with the prefrontal cortex (MFG; BA 9), visual analysis centers (MTG, ITG, fusiform gyrus), and a memory hub (parahippocampal gyrus); (2) the putamen and GP with the prefrontal cortex (SFG, IFG, preSMA) and visual processing areas (MTG); (3) the SMA with association centers (inferior parietal cortex); and (4) the right insula with visual processing (ITG) and attention centers (superior parietal cortex). In the PD group, connectivity of these seeds typically did not differ between the two timing conditions (Fig. 4A, dotted lines) or was weaker for AV than unimodal timing. Stronger connectivity for AV than for unimodal timing in the PD group relative to the control group was less common (Table 4; Fig. 4B). This pattern of results was found for (1) the right GP with the right caudate tail; (2) the right preSMA with the posterior insula, (3) the right insula with the medial SFG, and (4) the left cerebellum with the right SFG. In the control group, connectivity for some of these seeds (preSMA and cerebellum) was weaker for AV than for unimodal timing, whereas for other seeds (right GP, right insula, and right IFG) connectivity did not differ between the timing conditions (Fig. 4B, dotted lines). Thus, when the integration of audiovisual temporal codes was thought to be more attention demanding, timing impairments in patients were especially linked to a weakening in CTBG connectivity with widespread anterior and posterior cortical regions. Unlike

controls, PD patients were unable to flexibly increase the strength of normal CTBG interactions with the cortex. A similar connectivity pattern was also found for the insula, yet cerebellar connectivity with the frontal cortex was notably enhanced in patients.

In contrast, connectivity of the CTBG circuit, the anterior insula, and the cerebellum was stronger for VA than for unimodal timing largely in the PD group (Table 5; Fig. 4D). Connectivity of these seeds was notably stronger with areas of the prefrontal cortex. This included stronger VA connectivity for: (1) the caudate head and body with prefrontal cortex (IFG and MFG); (2) the SMA and preSMA with the caudate tail; (3) the right insula with a visual center (lingual gyrus); and (4) the left cerebellum with right prefrontal cortex (IFG, SFG). In the control group, connectivity of over 50% of these seed-target regions did not did not differ between the timing conditions (Fig. 4D, dotted lines), and for the remaining seeds connectivity was weaker for VA than for unimodal timing. Stronger connectivity for VA than for unimodal timing in the control group relative to the PD group was uncommon (Table 5; Fig. 4C), but was found for the: (1) right caudate head with posterior cingulate; (2) right preSMA with the rostral prefrontal cortex (left SFG); and (3) left cerebellum with the left culmen and a visual center (lingual gyrus). For the PD group, connectivity in these regions did not differ between the timing conditions (Fig. 4C, dotted lines) except for the cerebellum, wherein connectivity was stronger for unimodal than VA timing. Thus, when the integration of audiovisual temporal codes was thought to be less attention demanding, enhanced connectivity of the CTBG, insula and cerebellum was prominent in PD, particularly with the frontal cortices and the caudate tail.

3.4. Discriminant Analyses with Classifijication

Next, we sought to identify the sensitivity and specificity of the fMRI measures that showed group differences by using a stepwise discriminant analysis with leave-one out cross-validation. The discriminant analysis identified the linear combination of fMRI measures that best classified subjects into their respective groups. Cross validation of the discriminant function was conducted in multiple tests by leaving each subject out of the analyses. In the conventional regional analyses that compared the groups in the difference between the magnitude of activation for AV versus unimodal timing (Table 2), right anterior insula activation best discriminated between the groups, correctly classifying a total of 66.7% of the subjects into their actual group. The sensitivity of this measure was moderate, correctly classifying 70.4% of the PD patients; however, specificity was poor with only 62.5% of the controls subjects correctly classified.

Classification accuracy using the PPI-based network connectivity measures was considerably better. For the measures associated with stronger AV connectivity, the sensitivity and specificity of the discriminant function was high, correctly classifying 88.9% of the PD patients and 87.5% of the controls, respectively (total classification accuracy = 88.2%). Only one PD patient and three controls were misclassified. For the measures associated with stronger VA connectivity, sensitivity was excellent, with 100% of the PD patients correctly classified; specificity was high with 87.5% of the controls correctly classified (total classification accuracy = 94.1%). For both crossmodal conditions, network measures that showed stronger connectivity in the control or in the PD groups both

contributed to the classification function. Table 6 shows that CTBG and left cerebellum connectivity were the best discriminating network measures for both classification analyses, although connectivity of the right anterior insula with the right medial SFG also contributed to the AV classification results. Measures of timing accuracy did not add to or improve the classification results. These results demonstrated that measures of network connectivity were far superior to measures of regional activation in predicting group membership.

Partial correlations showed that greater expression of both discriminant functions (i.e., greater functional connectivity disturbances) was associated with a longer disease duration (unimodal versus AV: $r_{age} = 0.38$, $p = 0.05$; unimodal versus VA: $r_{age} = 0.46$, $p = 0.018$), but not levodopa dosage equivalence ($p > 0.80$) or the severity of motor symptoms OFF medication (total UPDRS motor score, $p > 0.30$). These results suggest network connectivity measures were not related to motor functioning.

3.5. Structural MRI and Correlation with fMRI Data

T tests for group differences in cortical, cerebellar, CSF, thalamus, and globus pallidus volumes were nonsignificant. However, caudate and putamen volumes were significantly reduced in the PD group relative to controls (Table 7). In PD, caudate and putamen volumes were not significantly correlated with activation of the fROI in Table 2 or with any of the PPI-based effective connectivity measures. These results suggest that the amount of basal ganglia atrophy observed in PD patients in the current study does not account for the functional abnormalities that were associated with audiovisual timing deficits.

4. Discussion

Our study demonstrated that the presumed attention demands of the stimulus modality governed abnormalities in the synthesis of intersensory time-codes in PD and in underlying neuronal dysfunction. PD patients progressively underestimated intervals as their duration increased in both crossmodal conditions, consistent with a slowing in the accumulation rate of pulses by the clock process. However, impaired timing was more striking in the AV condition, where the resolution of visual time-codes purportedly depends more on controlled attention (Berry et al., 2014; Lustig & Meck, 2011). More subtle timing impairments in PD were found in the VA condition, despite the salience of auditory signals, which helps sustain attention to time (Berry et al., 2014). These findings could not be attributed to sensory deficits, as unimodal timing was normal in PD for both stimulus modalities, contrary to several studies (Artieda et al., 1992; Harrington et al., 1998, 2011b; Koch et al., 2004a, b; Malapani et al., 2002; Pastor et al., 1992; Rammsayer & Classen, 1997; Riesen & Schnider, 2001). Although the reasons for this discrepancy are not clear, heterogeneity in temporal processing proficiency in PD has been reported (Merchant et al., 2008a), and may be associated with a host of factors including individual differences in day-to-day symptom fluctuations, lingering effects of dopamine medications after overnight withdrawal, and disease severity. Our results suggest that intersensory timing is a more sensitive probe for dysfunction in PD, possibly owing to its emphasis on striatal integration of multisensory cortical oscillatory patterns. Intersensory timing impairments in PD were associated with abnormal regional activation of the CTBG, anterior insula, and inferior cerebellum, but only

when timing putatively required controlled attention. Most importantly, the patterns of abnormal functional connectivity of these brain regions differed in PD between the two intersensory timing conditions, and discriminated patients and healthy controls with high levels of sensitivity and specificity.

4.1. Abnormal Regional Activation During Controlled Timing in PD

Group differences in the amplitude of activation were observed only for the unimodal–AV comparison. Here, the PD group typically failed to modulate activity of the striatum, the globus pallidus, the anterior insula, and the inferior cerebellum in accord with the timing condition. An exception was activation of the left caudate head, which was greater for AV than unimodal timing. In contrast, activation in the control group was greater for unimodal than AV timing for all of these fROI, similar to young adults (Harrington et al., 2011a). Though these regions have all been implicated in temporal processing (Merchant et al., 2013a), their precise role is not well understood. By one model, timing emerges via striatal detection and integration of cortical oscillatory activity, which evolves as a function of event duration and thus, serves as the clock signal (Matell & Meck, 2004). The anterior insula, which is an element of the ventral attention system, is thought to assist with a bottom-up perceptual analysis of sensory information (Eckert et al., 2009), including temporal features (Kosillo & Smith, 2010; Livesey et al., 2007; Wittmann et al., 2010). Our results suggest that in PD the basal ganglia and insula fail to adapt to the increased integration and/or attentional demands when intersensory timing requires controlled attention. This includes the cerebellum, which by way of anatomical pathways to and from the basal ganglia (Bostan et al., 2010), may be a compensatory route for timing in PD (Kotz & Schwartze, 2011), possibly owing to its role in prediction and fine tuning of behavioral states.

Surprisingly, none of the above regions showed differential activation in the unimodal–VA comparison in either group. This finding indicates that when the audiovisual pairing of signals is thought to be more salient, activation of the basal ganglia, the anterior insula, and the inferior cerebellum is maintained at similar levels as when timing unimodal signals (Harrington et al., 2004, 2010; Rao et al., 2001). Although the amplitude of activation differed between the unimodal condition and each of the crossmodal timing conditions in other regions involved in timing (e.g., SMA, inferior frontal gyrus), including association areas (superior temporal and occipital cortices), activation patterns were remarkably normal in PD patients, despite subtle deficits in VA timing.

4.2. Functional Connectivity Disturbances in PD

Connectivity disturbances of the CTBG circuit, the anterior insula, and the inferior cerebellum were also examined in PD patients, since the experience of time emerges from interactions among different brain regions (Merchant et al., 2013a). Our results showed a striking dissociation between the groups in the connectivity of these regions for the time compression and the dilation conditions in comparison to unimodal timing.

When intersensory timing emphasized controlled attention (AV), connectivity of almost all elements of the CTBG circuit and the right anterior insula was typically stronger in the control group than in the PD group. Basal ganglia connectivity was stronger with cognitive-

control (inferior, middle, and superior frontal cortex; preSMA), ventral attention (middle and inferior temporal cortex, fusiform gyrus), and memory (parahippocampus) centers. Both the SMA and insula showed stronger connectivity with the dorsal-attention network (inferior and superior parietal cortex); insula connectivity was also stronger with the ventral-attention network (inferior temporal cortex). These connectivity patterns in PD patients were either weakened for controlled timing or altogether absent. This result points to a context-specific functional weakening or disconnection of the core timing system and the insula with frontal cognitive-control centers (Badre, 2008) and with the ventral-and dorsal-attention networks (Corbetta & Shulman, 2002). PD patients were unable to increase the strength of normal CTBG and insula interactions with the cortex, which may promote distractibility (Lee et al., 2010) and lead to a loss in the accumulation of pulses for visual information. Although stronger connectivity in the PD than in the control group was uncommon, connectivity of the cerebellum and the anterior insula with the lateral and medial superior-frontal cortices was notably enhanced in PD patients. The insula supports bottom-up attention to stimuli, which influences the experience of time (Dirnberger et al., 2012; Wittmann et al., 2010), such that enhanced connectivity with frontal cognitive-control centers may compensate for the increased attentional demands of timing visual signals. Enhanced cerebellar connectivity was also noteworthy, given the hyperactivity of the cerebellum in PD patients when timing movements (Jahanshahi et al., 2010; Yu et al., 2007). Enhanced functional connectivity of the cerebellum, often with motor areas, is also common in PD when performing motor tasks (Palmer et al., 2010; Wu et al., 2010a, b, 2011). Although these findings are often attributed to compensation by the cerebellum for deficient basal ganglia functioning (Merchant et al., 2013a), it is unknown if the cerebellum substitutes for deficiencies in the striatal timing-system by improving behavioral states.

These findings contrasted with the salient intersensory condition (VA), wherein connectivity of certain elements of the CTBG circuit, the anterior insula, and the left cerebellum was typically stronger in the PD than in the control group. Cerebellum connectivity with the lateral superior frontal cortex was enhanced in PD, as it was for controlled timing, but so was connectivity with an inhibitory hub, namely the right inferior frontal gyrus (Aron & Poldrack, 2006), that is commonly engaged during interval timing (Harrington et al., 2010; Merchant et al., 2013a). Of particular note was that caudate connectivity was stronger with cognitive-control centers (inferior and middle-frontal cortex), whereas SMA and preSMA connectivity were both stronger with the caudate tail. Interestingly, activity of the caudate is influenced by the saliency of stimuli (Zink et al., 2006), which is relevant to the prominence of auditory signals in the context of timing and to impaired saliency processing in PD (Mannan et al., 2008). Though stronger connectivity in the control group was uncommon for this condition, connectivity of the preSMA with a cognitive-control center (rostral lateral superior frontal cortex), the caudate head with a memory retrieval hub(posterior cingulate), and the inferior cerebellum with the culmen and a ventral-attention visual center (lingual gyrus) was stronger in the control group than in the PD group. Thus, subtle impairments in PD for less controlled temporal processing were associated with patterns of both enhanced and weakened connectivity of the caudate, SMA/preSMA and cerebellum. These disturbances may signify difficulties in temporal integration and sustained attention, even to auditory signals.

4.3. Sensitivity and Specifijicity of Regional Activation and Functional Connectivity

We also found that measures of functional connectivity better distinguished PD patients from control subjects than conventional measures of regional-activation amplitude. This finding is consistent with emerging research in PD showing that measures of functional connectivity can be more sensitive than regional activation to changes in brain networks in a disease, especially in earlier stages (Harrington et al., 2011b; Rowe, 2010), and to the effects of pharmacotherapy (Harrington et al., 2011b; Rowe et al., 2010). This is because regional activation overlooks interactions among brain regions, which behaviors depend upon. In the present study, the sensitivity of the discriminant functions that best classified subjects into their respective groups was excellent, correctly classifying all (VA condition) or all but one (AV condition) PD patient. Specificity was also high, with only three control subjects misclassified. For controlled timing, the discriminant function included measures of weakened basal ganglia connectivity with cognitive-control (superior frontal), memory (parahippocampus), and ventral attention systems (middle temporal gyrus) and of enhanced insula and cerebellar connectivity with cognitive-control systems (rostral lateral and medial superior-frontal) in PD patients. For salient timing, the discriminant function was comprised of caudate, SMA/preSMA, and cerebellum connectivity patterns that were both weakened and enhanced in PD patients, particularly with cognitive-control systems (rostral superior-frontal) and the caudate tail. These findings further highlighted the dissociation between controlled and salient intersensory timing, especially in the expression of CTBG dysfunction, possibly suggesting that context-dependent dynamic patterns within this circuit govern the resolution of perceived duration. An exception was the weakened connectivity in PD of the right caudate head with elements of a memory system (parahippocampus or posterior cingulate) for both discriminant functions, which comports with temporal-memory storage and retrieval dysfunction in PD (Harrington et al., 2011b; Malapani et al., 2002). The prominence of CTBG, insula, and cerebellar connectivity disturbances with the rostral superior-frontal cortices was also notable since these areas modulate the dilation of time caused by stimuli that have an emotional connotation (Dirnberger et al., 2012; Wittmann et al., 2010). This may relate to their role in stimulus-orientated attention (medial rostral prefrontal cortex) and self-maintained attention to thought (lateral rostral prefrontal cortex) (Burgess et al., 2007), which could both influence the resolution of time.

The expression of both discriminant functions did not correlate with motor symptom severity, in support of their cognitive basis. This finding contrasts with studies of motor control, wherein functional connectivity of the CTBG system and the cerebellum correlate with motor symptom severity (Wu et al., 2010a, 2011). Rather, greater expression of abnormal network connectivity correlated with longer disease duration, suggesting that functional connectivity disturbances in timing-related systems may have the potential to track changes in cognitive brain networks in PD. Longitudinal studies will be needed to address this possibility and to evaluate the prognostic value of measures of network expression in predicting the development of clinically significant cognitive impairment, especially in executive functions and attention.

4.4. Summary

We found for the first time that context-dependent patterns of weakened and enhanced functional connectivity in PD were striking within a presumed core timing system (CTBG circuit) and an element of the ventral attention network (anterior insula), whereas cerebellar connectivity was enhanced irrespective of the putative attention demands of intersensory timing. Although the selection of regions for our connectivity analyses was driven by timing theory, past research, and regional activation abnormalities found in PD patients by the present study, the connectivity patterns that we identified for different intersensory timing conditions may not represent a complete account of all networks that govern context-specific interval timing (Salvioni et al., 2013; Wiener et al., 2011). As such, impaired audiovisual timing in PD may also relate to changes in other brain networks. Nonetheless, multivariate combinations of abnormal network expression showed excellent specificity and sensitivity, suggesting that CTBG, insula, and cerebellar connectivity well characterized intersensory timing dysfunction in PD. Validation of the network expression measures in other samples will be critical to evaluate their potential as surrogate markers of brain functioning that could be used for clinical applications. Lastly, although distortions in audiovisual timing are commonly attributed to attention factors, this hypothesis requires further validation. Of relevance here is recent monkey research reporting that visual and auditory interval markers have a differential effect on interval tuning in the CTBG (i.e., SMA and preSMA) that cannot be attributed to attention (Merchant et al., 2013b). Thus, the differential patterns of CTBG connectivity disturbances in PD patients for AV and VA timing may be partly related to changes in more basic neuronal processes. Future studies with larger samples and a wider range of performances on measures of attention and executive functioning than for the present study may be helpful in unraveling potential cognitive factors that underlie changes in networks associated with impaired audiovisual timing in PD.

Acknowledgements

This research was funded by a grant from the Department of Veterans Affairs to D. L. Harrington (CX000146). The authors would like to thank Dr. Alan Simmons and Christopher Fong for their technical assistance on various aspects of the study.

References

Agostino PV, Golombek DA, & Meck WH (2011). Unwinding the molecular basis of interval and circadian timing. Front. Integr. Neurosci, 5, 64. [PubMed: 22022309]

Aron AR, & Poldrack RA (2006). Cortical and subcortical contributions to Stop signal response inhibition: Role of the subthalamic nucleus. J. Neurosci, 26, 2424–2433. [PubMed: 16510720]

Artieda J, Pastor MA, Lacruz F, & Obeso JA (1992). Temporal discrimination is abnormal in Parkinson’s disease. Brain, 115, 199–210. [PubMed: 1559154]

Badre D (2008). Cognitive control, hierarchy, and the rostro-caudal organization of the frontal lobes. Trends Cogn. Sci, 12, 193–200. [PubMed: 18403252]

Balci F, Wiener M, Cavdaroglu B, & Branch CH (2013). Epistasis effects of dopamine genes on interval timing and reward magnitude in humans. Neuropsychologia, 51, 293–308. [PubMed: 22903038]

Berry AS, Li X, Lin Z, & Lustig C (2014). Shared and distinct factors driving attention and temporal processing across modalities. Acta Psychol. (Amst.), 147, 42–50. [PubMed: 23978664]

Bostan AC, Dum RP, & Strick PL (2010). The basal ganglia communicate with the cerebellum. Proc. Natl Acad. Sci. USA, 107, 8452–8456. [PubMed: 20404184]

Burgess PW, Dumontheil I, & Gilbert SJ (2007). The gateway hypothesis of rostral prefrontal cortex (area 10) function. Trends Cogn. Sci, 11, 290–298. [PubMed: 17548231]

Chen KM, & Yeh SL (2009). Asymmetric cross-modal effects in time perception. Acta Psychol. (Amst.), 130, 225–234. [PubMed: 19195633]

Corbetta M, & Shulman GL (2002). Control of goal-directed and stimulus-driven attention in the brain. Nat. Rev. Neurosci, 3, 201–215. [PubMed: 11994752]

Coull JT, Hwang HJ, Leyton M, & Dagher A (2012). Dopamine precursor depletion impairs timing in healthy volunteers by attenuating activity in putamen and supplementary motor area. J. Neurosci, 32, 16704–16715. [PubMed: 23175824]

Cox RW (1996). AFNI: Software for analysis and visualization of functional magnetic resonance neuroimages. Comput. Biomed. Res, 29, 162–173. [PubMed: 8812068]

Dirnberger G, Hesselmann G, Roiser JP, Preminger S, Jahanshahi M, & Paz R (2012). Give it time: Neural evidence for distorted time perception and enhanced memory encoding in emotional situations. Neuroimage, 63, 591–599. [PubMed: 22750720]

Eckert MA, Menon V, Walczak A, Ahlstrom J, Denslow S, Horwitz A, & Dubno JR (2009). At the heart of the ventral attention system: The right anterior insula. Hum. Brain Mapp, 30, 2530–2541. [PubMed: 19072895]

Fischl B, Liu A, & Dale AM (2001). Automated manifold surgery: Constructing geometrically accurate and topologically correct models of the human cerebral cortex. IEEE Trans. Med. Imaging, 20, 70–80. [PubMed: 11293693]

Fischl B, van der Kouwe A, Destrieux C, Halgren E, Segonne F, Salat DH, Busa E, Seidman LJ, Goldstein J, Kennedy D, Caviness V, Makris N, Rosen B, & Dale AM (2004). Automatically parcellating the human cerebral cortex. Cereb. Cortex, 14, 11–22. [PubMed: 14654453]

Friston KJ, Buechel C, Fink GR, Morris J, Rolls E, & Dolan RJ (1997). Psychophysiological and modulatory interactions in neuroimaging. Neuroimage, 6, 218–229. [PubMed: 9344826]

Gibbon J, Church RM, & Meck WH (1984). Scalar timing in memory. Ann. N. Y. Acad. Sci, 423, 52–77. [PubMed: 6588812]

Harrington DL, Boyd LA, Mayer AR, Sheltraw DM, Lee RR, Huang M, & Rao SM (2004). Neural representation of interval encoding and decision making. Cogn. Brain Res, 21, 193–205.

Harrington DL, Castillo GN, Fong CH, & Reed JD (2011a). Neural underpinnings of distortions in the experience of time across senses. Front. Integr. Neurosci, 5, 32. [PubMed: 21847374]

Harrington DL, Castillo GN, Greenberg PA, Song DD, Lessig S, Lee RR, & Rao SM (2011b). Neurobehavioral mechanisms of temporal processing deficits in Parkinson's disease. PLoS ONE, 6, e17461. [PubMed: 21364772]

Harrington DL, Haaland KY, & Hermanowicz N (1998). Temporal processing in the basal ganglia. Neuropsychology, 12, 3–12. [PubMed: 9460730]

Harrington DL, Zimbelman JL, Hinton SC, & Rao SM (2010). Neural modulation of temporal encoding, maintenance, and decision processes. Cereb. Cortex, 20, 1274–1285. [PubMed: 19778958]

Jahanshahi M, Jones CR, Zijlmans J, Katzenschlager R, Lee L, Quinn N, Frith CD, & Lees AJ (2010). Dopaminergic modulation of striato-frontal connectivity during motor timing in Parkinson's disease. Brain, 133, 727–745. [PubMed: 20305278]

Klink PC, Montijn JS, & van Wezel RJ (2011). Crossmodal duration perception involves perceptual grouping, temporal ventriloquism, and variable internal clock rates. Atten. Percept. Psychophys, 73, 219–236. [PubMed: 21258921]

Koch G, Brusa L, Caltagirone C, Oliveri M, Peppe A, Tiraboschi P, & Stanzione P (2004a). Subthalamic deep brain stimulation improves time perception in Parkinson's disease. NeuroReport, 15, 1071–1073. [PubMed: 15076737]

Koch G, Oliveri M, Brusa L, Stanzione P, Torriero S, & Caltagirone C (2004b). High-frequency rTMS improves time perception in Parkinson disease. Neurology, 63, 2405–2406. [PubMed: 15623713]

Kosillo P, & Smith AT (2010). The role of the human anterior insular cortex in time processing. Brain Struct. Funct, 214, 623–628. [PubMed: 20512365]

Kotz SA, & Schwartze M (2011). Differential input of the supplementary motor area to a dedicated temporal processing network: Functional and clinical implications. Front. Integr. Neurosci, 5, 86. [PubMed: 22363269]

Lake JI, & Meck WH (2013). Differential effects of amphetamine and haloperidol on temporal reproduction: dopaminergic regulation of attention and clock speed. Neuropsychologia, 51, 284–292. [PubMed: 22982605]

Lee EY, Cowan N, Vogel EK, Rolan T, Valle-Inc I, & Hackley SA (2010). Visual working memory deficits in patients with Parkinson's disease are due to both reduced storage capacity and impaired ability to filter out irrelevant information. Brain, 133, 2677–2689. [PubMed: 20688815]

Lee SJ, Yoo JY, Ryu JS, Park HK, & Chung SJ (2012). The effects of visual and auditory cues on freezing of gait in patients with Parkinson disease. Am. J. Phys. Med. Rehabil, 91, 2–11. [PubMed: 22157432]

Livesey AC, Wall MB, & Smith AT (2007). Time perception: Manipulation of task difficulty dissociates clock functions from other cognitive demands. Neuropsychologia, 45, 321–331. [PubMed: 16934301]

Lustig C, & Meck WH (2011). Modality differences in timing and temporal memory throughout the lifespan. Brain Cogn, 77, 298–303. [PubMed: 21843912]

Majsak MJ, Kaminski T, Gentile AM, & Flanagan JR (1998). The reaching movements of patients with Parkinson's disease under self-determined maximal speed and visually cued conditions. Brain, 121 (Pt 4), 755–766. [PubMed: 9577399]

Malapani C, Deweer B, & Gibbon J (2002). Separating storage from retrieval dysfunction of temporal memory in Parkinson's disease. J. Cogn. Neurosci, 14, 311–322. [PubMed: 11970794]

Mannan SK, Hodgson TL, Husain M, & Kennard C (2008). Eye movements in visual search indicate impaired saliency processing in Parkinson's disease. Prog. Brain Res, 171, 559–562. [PubMed: 18718353]

Matell MS, & Meck WH (2004). Cortico-striatal circuits and interval timing: Coincidence detection of oscillatory processes. Cogn. Brain Res, 21, 139–170.

Mayer AR, Franco AR, Canive J, & Harrington DL (2009). The effects of stimulus modality and frequency of stimulus presentation on cross-modal distraction. Cereb. Cortex, 19, 993–1007. [PubMed: 18787235]

McIntosh GC, Brown SH, Rice RR, & Thaut MH (1997). Rhythmic auditory-motor facilitation of gait patterns in patients with Parkinson's disease. J. Neurol. Neurosurg. Psychiatr, 62, 22–26.

Meck WH (1996). Neuropharmacology of timing and time perception. Cogn. Brain Res, 3, 227–242.

Merchant H, Harrington DL, & Meck WH (2013a). Neural basis of the perception and estimation of time. Annu. Rev. Neurosci, 36, 313–336. [PubMed: 23725000]

Merchant H, Luciana M, Hooper C, Majestic S, & Tuite P (2008a). Interval timing and Parkinson's disease: Heterogeneity in temporal performance. Exp. Brain Res, 184, 233–248. [PubMed: 17828600]

Merchant H, Perez O, Zarco W, & Gamez J (2013b).Interval tuningin the primatemedial premotor cortex as a general timing mechanism. J. Neurosci, 33, 9082–9096. [PubMed: 23699519]

Merchant H, Zarco W, & Prado L (2008b). Do we have a common mechanism for measuring time in the hundreds of millisecond range? Evidence from multiple-interval timing tasks. J. Neurophysiol, 99, 939–949. [PubMed: 18094101]

Nagy A, Eordegh G, Paroczy Z, Markus Z, & Benedek G (2006). Multisensory integration in the basal ganglia. Eur. J. Neurosci, 24, 917–924. [PubMed: 16930419]

Nieuwboer A, Vercruysse S, Feys P, Levin O, Spildooren J, & Swinnen S (2009). Upper limb movement interruptions are correlated to freezing of gait in Parkinson's disease. Eur. J. Neurosci, 29, 1422–1430. [PubMed: 19309319]

Palmer SJ, Li J, Wang ZJ, & McKeown MJ (2010). Joint amplitude and connectivity compensatory mechanisms in Parkinson's disease. Neuroscience, 166, 1110–1118. [PubMed: 20074617]

Pastor MA, Artieda J, Jahanshahi M, & Obeso JA (1992). Time estimation and reproduction is abnormal in Parkinson's disease. Brain, 115, 225.

Penney TB, Gibbon J, & Meck WH (2000). Differential effects of auditory and visual signals on clock speed and temporal memory. J. Exp. Psychol. Hum. Percept. Perform, 26, 1770–1787. [PubMed: 11129373]

Rammsayer T, & Classen W (1997). Impaired temporal discrimination in Parkinson's disease: Temporal processing of brief durations as an indicator of degeneration of dopaminergic neurons in the basal ganglia. Int. J. Neurosci, 91, 45–55. [PubMed: 9394214]

Rao SM, Mayer AR, & Harrington DL (2001). The evolution of brain activation during temporal processing. Nat. Neurosci, 4, 317–323. [PubMed: 11224550]

Razmy A, Lang AE, & Shapiro CM (2004). Predictors of impaired daytime sleep and wakefulness in patients with Parkinson disease treated with older (ergot) vs newer (nonergot) dopamine agonists. Arch. Neurol, 61, 97–102. [PubMed: 14732626]

Repp BH, & Penel A (2002). Auditory dominance in temporal processing: New evidence from synchronization with simultaneous visual and auditory sequences. J. Exp. Psychol. Hum. Percept. Perform, 28, 1085–1099. [PubMed: 12421057]

Riesen JM, & Schnider A (2001). Time estimation in Parkinson's disease: Normal long duration estimation despite impaired short duration discrimination. J. Neurol, 248, 27–35. [PubMed: 11266017]

Rowe JB (2010). Connectivity analysis is essential to understand neurological disorders. Front. Syst. Neurosci, 4, 144. [PubMed: 20948582]

Rowe JB, Hughes LE, Barker RA, & Owen AM (2010). Dynamic causal modelling of effective connectivity from fMRI: Are results reproducible and sensitive to Parkinson's disease and its treatment? Neuroimage, 52, 1015–1026. [PubMed: 20056151]

Salvioni P, Murray MM, Kalmbach L, & Bueti D (2013). How the visual brain encodes and keeps track of time. J. Neurosci, 33, 12423–12429. [PubMed: 23884947]

Spildooren J, Vercruysse S, Meyns P, Vandenbossche J, Heremans E, Desloovere K, & Vanden-berghe W (2012). Turning and unilateral cueing in Parkinson's disease patients with and without freezing of gait. Neuroscience, 207, 298–306. [PubMed: 22285883]

Ulrich R, Nitschke J, & Rammsayer T (2006). Crossmodal temporal discrimination: Assessing the predictions of a general pacemaker-counter model. Percept. Psychophys, 68, 1140–1152. [PubMed: 17355038]

Vercruysse S, Spildooren J, Heremans E, Vandenbossche J, Wenderoth N, Swinnen SP, Vanden-berghe W, & Nieuwboer A (2012). Abnormalities and cue dependence of rhythmical upper-limb movements in Parkinson patients with freezing of gait. Neurorehabil. Neural Repair, 26, 636–645. [PubMed: 22291041]

Wearden JH, Edwards H, Fakhri M, & Percival A (1998). Why "sounds are judged longer than lights": Application of a model of the internal clock in humans. Q. J. Exp. Psychol. B, 51, 97–120. [PubMed: 9621837]

Wiener M, Matell MS, & Coslett HB (2011). Multiple mechanisms for temporal processing. Front. Integr. Neurosci, 5, 31. [PubMed: 21808611]

Wittmann M, van Wassenhove V, Craig AD, & Paulus MP (2010). The neural substrates of subjective time dilation. Front. Hum. Neurosci, 4, 2. [PubMed: 20161994]

Wu T, Chan P, & Hallett M (2010a). Effective connectivity of neural networks in automatic movements in Parkinson's disease. Neuroimage, 49, 2581–2587. [PubMed: 19853664]

Wu T, Wang L, Hallett M, Chen Y, Li K, & Chan P (2011). Effective connectivity of brain networks during self-initiated movement in Parkinson's disease. Neuroimage, 55, 204–215. [PubMed: 21126588]

Wu T, Wang L, Hallett M, Li K, & Chan P (2010b). Neural correlates of bimanual anti-phase and in-phase movements in Parkinson's disease. Brain, 133, 2394–2409. [PubMed: 20566485]

Yu H, Sternad D, Corcos DM, & Vaillancourt DE (2007). Role of hyperactive cerebellum and motor cortex in Parkinson's disease. Neuroimage, 35, 222–233. [PubMed: 17223579]

Zink CF, Pagnoni G, Chappelow J, Martin-Skurski M, & Berns GS (2006). Human striatal activation reflects degree of stimulus saliency. Neuroimage, 29, 977–983. [PubMed: 16153860]

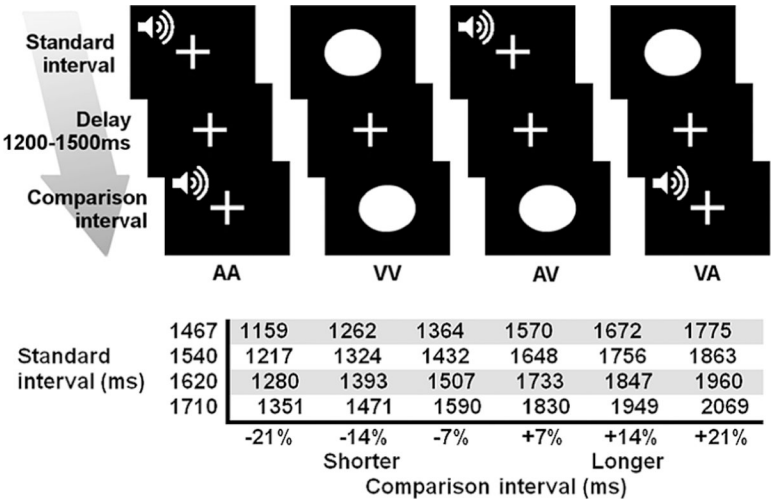

Figure 1.

Time perception task and experimental conditions. (Top) Subjects fixated on a crosshair throughout the experiment. Pairs of auditory (A) and visual stimuli (V) were successively presented. Standard and comparison intervals were of the same (AA, VV) or different modality (AV, VA). (Bottom) For each standard interval, there were three shorter and three longer comparison intervals.

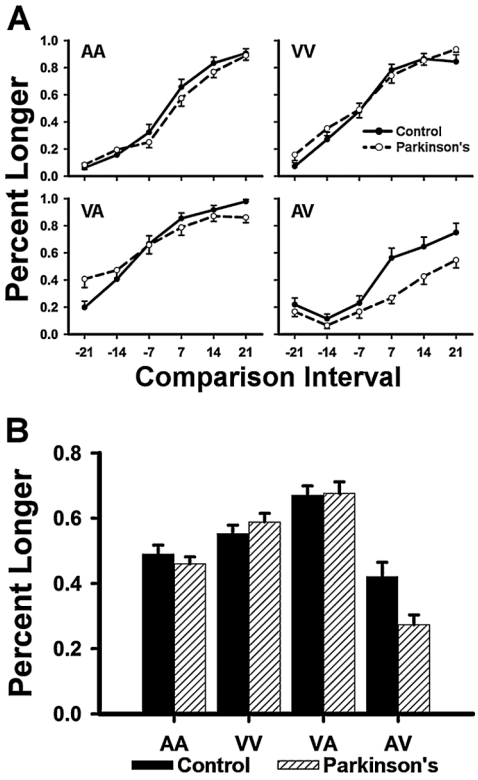

Figure 2.

Task performance. Mean (standard error bars) percent longer responses for the control and the Parkinson's groups. (A) Group × comparison interval interaction. Comparison intervals are ±7, 14, and 21% shorter/longer than the SI. (B) Group × timing condition × comparison interval modality interaction. A = auditory; V = visual.

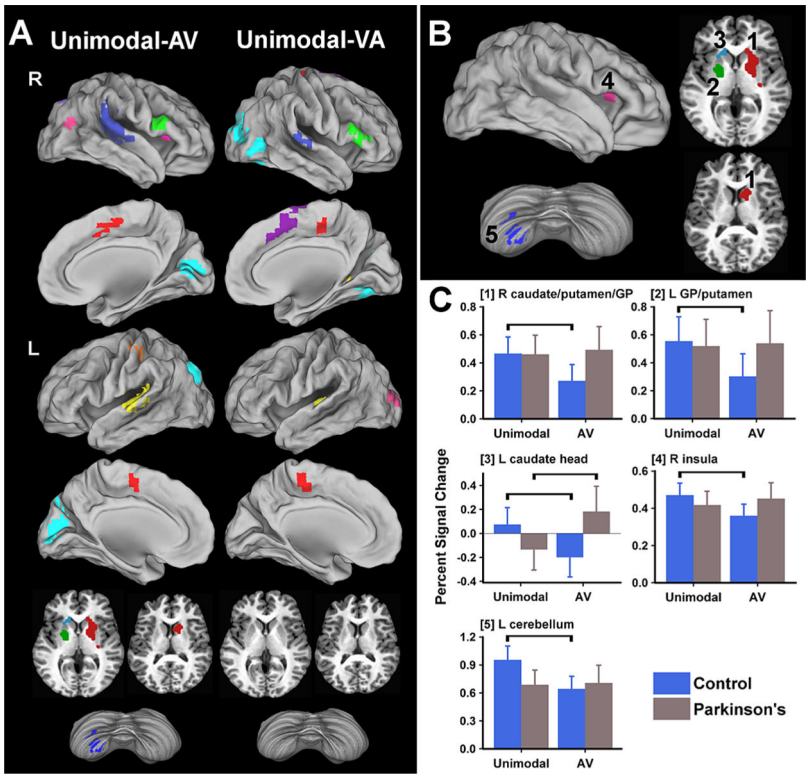

Figure 3.

Effects of timing condition on regional brain activation. (A) fROI showing a main effect of timing condition for the unimodal–AV (auditory–visual pairs) and the unimodal–VA (visual–auditory pairs) subtractions. Colors demarcate the different fROI associated with each contrast. The first four rows display sagittal views of cortical fROI in the right (R) and left (L) hemisphere. Axial views of the basal ganglia and cerebellum are displayed at the bottom. Tables 2 and 3 detail the brain regions, spatial coordinates, and volumes of these clusters. (B) fROI demonstrating significant group × timing condition interactions for the unimodal–AV subtraction. These regions are designated by superscript numbers in Table 2. (C) Bar graphs display the mean (standard error bars) percent signal change for each fROI shown in Fig. 3B (numbers in brackets correspond to the fROI shown in the figure). Horizontal lines designate significant differences between the unimodal and AV conditions for each group. GP = globus pallidus. This figure is published in colour in the online version.

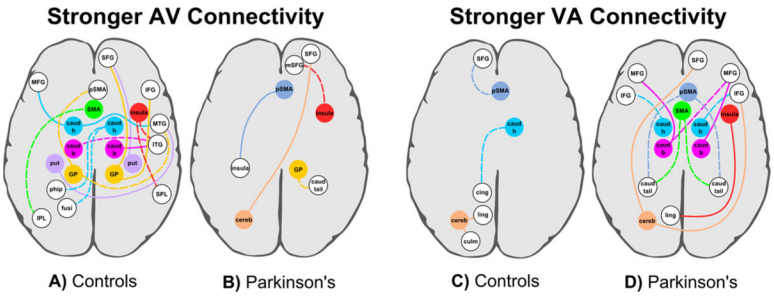

Figure 4.

Network connectivity maps. Group differences in connectivity of a seed (colored circles and lines) with other brain regions (white circles). Dotted lines indicate that connectivity was not modulated by a seed ROI for the other group. (A, B) Stronger connectivity for AV than unimodal timing (A) in the control than the PD group and (B) in the PD than the control group. Table 4 describes the seed/brain regions, spatial coordinates, and volumes. (C, D) Stronger connectivity for VA than unimodal timing (C) in the control than the PD group and (D) in the PD than the control group. Table 5 describes the seed/brain regions, spatial coordinates, and volumes. caud b, h, tail = caudate body, head, tail; cereb = cerebellum; cing = cingulate; culm = culmen; fusi = fusiform; GP = globus pallidus; IFG inferior frontal; IPL inferior parietal; ITF = inferior temporal; ling = lingual; MFG = middle frontal; MTG = middle temporal; mSFG = medial superior frontal; phip = parahippocampus; pSMA = preSMA; put = putamen; SFG = superior frontal; SMA = supplementary motor area; SPL = superior parietal; thal = thalamus. This figure is published in colour in the online version.

Table 1.

Characteristics of the PD and the control groups

	Control	PD	*t* value	*p*
Demographics				
Age	64.3 (8.2)	65.6 (7.9)	−0.43	0.70
Education (years)	17.4 (2.7)	16.4 (2.2)	1.40	0.17
% Male[1]	58%	48%		0.47
Mini Mental Status Exam	29.1 (0.9)	28.9 (1.2)	0.65	0.52
Executive Functions				
Stroop Interference	50.9 (6.4)	49.5 (6.1)	0.79	0.43
DKEFS Letter Fluency[2]	13.4 (3.5)	11.4 (3.3)	2.16	0.04
DKEFS Category Fluency[2]	12.0 (4.3)	10.5 (3.5)	1.39	0.17
Trial Making Test Part A	9.1 (2.1)	8.3 (2.3)	1.31	0.22
Trail Making Test Part B	10.1 (2.3)	9.9 (2.6)	0.10	0.92
Visual Cognition				
Line Orientation	26.8 (2.1)	25.3 (3.6)	1.38	0.17
Memory				
WAIS III: Digit Span Total[3]	11.7 (2.2)	11.9 (2.6)	0.11	0.91
WAIS III: Spatial Span Total[3]	15.5 (4.4)	16.2 (2.7)	−0.64	0.53
CVLT Immediate Free Recall	60.2 (10.5)	56.6 (9.1)	1.29	0.20
CVLT Long Delay Free Recall	0.75 (0.68)	0.48 (0.70)	1.39	0.17

For most neuropsychological tests, values are scaled score means (standard deviations). *T* scores are reported for Stroop Interference and the California Verbal Learning Test (CVLT) Immediate Free Recall. Standard scores are reported for the CVLT Long Delay Free Recall.

[1]Chi-Square Test.

[2]Delis–Kaplan Executive Function System (DKEFS).

[3]Wechsler Adult Intelligence Scale (WAIS) third edition.

Table 2.

Regions showing differences in activation between the unimodal and AV timing conditions in one or both groups

	BA	ml	*x*	*y*	*z*
Unimodal < AV					
Bilateral cuneus, precuneus, angular gyrus	7, 18, 39	13.12	−11	−74	20
Right precuneus	7	1.47	24	−57	40
Right middle temporal	39	1.22	44	−65	17
Unimodal > AV					
Bilateral SMA, cingulate	6, 24	3.52	4	−1	48
Left precentral/postcentral	3, 4	2.11	−37	−21	49
Right inferior frontal	44	3.07	49	13	18
Right superior temporal	22, 41, 42	11.71	53	−24	11
Left superior temporal	22, 41	7.81	−47	−25	10
[4] Right anterior insula	13	3.39	23	22	14
[1] Right caudate body, putamen, globus pallidus		4.67	19	5	8
[2] Left putamen, globus pallidus		1.28	−20	−5	7
[3] Left caudate head		0.64	−15	21	4
[5] Left inferior semi-lunar lobule		1.15	−21	−56	−46

fROI showing greater activation for AV than unimodal timing and greater activation for unimodal than AV timing. Spatial maps of the regions are displayed in the first column of Fig. 3A. BA = Brodmann area. Main effects of group were not significant for any of the regions.

[1–5]Regions with a superscript number are those showing a significant group × timing condition interaction ($p < 0.05$, FDR corrected). All of these fROI showed significantly greater activation in the unimodal than in the AV condition (AAVV > AV) in the control group, but not in the PD group. An exception was the left caudate head, which showed greater MR signal intensity for the AV than the unimodal condition in the PD group. No other group effects were found.

Table 3.

Regions showing differences in activation between the unimodal and VA timing conditions in both groups

	BA	ml	*x*	*y*	*z*
Unimodal < VA					
Right superior temporal	22	2.05	55	−21	8
Left superior temporal	41	1.47	−46	−23	8
Unimodal > VA					
Right preSMA, cingulate	6, 32	3.71	7	10	51
Bilateral SMA, cingulate	6, 24	4.61	2	−20	51
Right inferior frontal	44, 45	2.05	50	26	14
Right middle occipital, lingual gyrus, fusiform gyrus, occipitotemporal	19, 37	13.25	31	−71	7
Left middle occipital	18	3.58	−23	−86	13
Right parahippocampus, thalamus, pulvinar		1.92	21	−35	6

fROI showing greater activation for VA than unimodal timing and greater activation for unimodal than VA timing. Spatial maps of the regions are displayed in the second column of Fig. 3A. BA = Brodmann area. Main effects of group and group × timing conditions interactions were not significant for any of the regions.

Table 4.

Group differences in effective connectivity: AV versus unimodal timing

Seed	Region	ml	*x*	*y*	*z*
AV STRONGER IN CONTROLS					
R caudate head	L parahippocampal gyrus[a]	0.58	−32	−38	−10
	L fusiform gyrus[a]	0.51	−34	−58	−7
L caudate head	L MFG (BA 9)	0.90	−30	28	31
	R MTG (BA 21)	0.58	56	−18	−14
R caudate body	R ITG (BA 20)	0.96	57	−23	−17
L caudate body	R ITG[a] (BA 20)	0.83	56	−23	−15
R putamen	R SFG (BA 8)	2.75	9	38	42
L putamen	R MTG (BA 21)	0.77	56	−23	−12
R GP	R SFG (BA 8)	3.33	6	39	40
	R IFG (BA 44)	0.70	42	39	−1
L GP	R MTG[a] (BA 21)	1.47	60	−22	−12
	R preSMA[a] (BA 6)	0.51	6	34	35
B SMA	L IPL[a] (BA40)	1.41	−42	−54	41
R insula	R ITG[a] (BA 20)	0.83	59	−23	−15
	R SPL[a] (BA 7)	0.64	29	−62	53
AV STRONGER IN PD					
R GP	R caudate tail[b]	0.83	19	−36	19
R preSMA	L posterior insula (BA 13)	1.54	−24	−31	22
R insula	R medial SFG[b] (BA 10)	0.58	7	65	−6
L cerebellum (inferior semi-lunar lobule)	R SFG (BA 10)	1.92	23	44	23

Significant group differences in effective connectivity of a seed with a brain region (FDR adjusted).

[a]Connectivity was not modulated by the timing condition in the PD group.

[b]Connectivity was not modulated by the timing condition in the control group.

B = bilateral; BA = Brodmann area; GP = globus pallidus; IFG = inferior frontal gyrus; IPL = inferior parietal lobule; ITG = inferior temporal gyrus; L = left; MFG = middle frontal gyrus; MTG = middle temporal gyrus; R = right; SFG = superior frontal gyrus; SMA = supplementary motor area; SPL = superior parietal lobule.

Table 5.

Group differences in effective connectivity: VA versus unimodal timing

Seed	Region	ml	*x*	*y*	*z*
VA STRONGER IN CONTROLS					
R caudate head	L posterior cingulate[a] (BA 23)	0.70	−16	−54	26
R preSMA	L SFG[a] (BA 10)	0.64	−18	48	−13
L inferior semi-lunar lobule	L culmen	3.14	−16	−49	−15
	L lingual gyrus (BA 18)	0.83	−11	−67	−5
VA STRONGER IN PD					
R caudate head	R IFG[b] (BA 9)	0.83	53	14	30
L caudate head	L IFG[b] (BA 45)	0.64	−50	17	18
R caudate body	R MFG (BA 9)	1.41	50	17	29
L caudate body	L MFG (BA 46)	1.02	−45	18	25
	R MFG[b] (BA 9)	0.90	51	18	30
B SMA	R caudate tail[b]	1.41	16	−36	15
	L caudate tail[b]	0.90	−19	−34	20
R preSMA	L caudate tail[b]	1.22	−23	−33	20
	R caudate tail[b]	0.77	16	−37	16
R insula	L lingual gyrus (BA 18)	0.64	−12	−98	−10
L cerebellum (inferior semi-lunar lobule)	R IFG (BA9)	0.90	57	8	29
	R SFG (BA 10)	0.51	25	45	22

Significant group differences in effective connectivity of a seed with a brain region (FDR adjusted).

[a]Connectivity was not modulated by the timing condition in the PD group.

[b]Connectivity was not modulated by the timing condition in the control group.

B = bilateral; BA = Brodmann area; IFG = inferior frontal gyrus; L = left; MFG = middle frontal gyrus; R = right; SFG = superior frontal gyrus; SMA = supplementary motor area.

Table 6.

Standardized canonical discriminant function coefficients (SCDFC) for PPI-based network connectivity measures that uniquely discriminated between the PD and control groups

STRONGER AV CONNECTIVITY		STRONGER VA CONNECTIVITY	
Seed/Region	**SCDFC**	**Seed/Region**	**SCDFC**
R caudate head/L parahippocampus[a]	0.392	R caudate head/L posterior cingulate (BA 23)[a]	0.725
R putamen/R SFG (BA 8)[a]	0.526	R preSMA/L SFG (BA 10)[a]	0.739
L GP/R MTG (BA 21)[a]	0.368	L cerebellum/L culmen[a]	0.605
R insula/R mSFG (BA 10)[b]	−0.445	L caudate body/L IFG (BA 45)[b]	−0.542
L cerebellum/R SFG (BA 10)[b]	−0.527	B SMA/L caudate tail[b]	−0.892
		R preSMA/R caudate tail[b]	0.533
		L cerebellum/R SFG (BA 10)[b]	−0.370

Group centroids were −1.493 (control group) and 1.327 (PD group) for the AV versus unimodal analyses and −2.106 (control group) and 1.872 (PD group) for the VA versus unimodal analyses.

[a]Stronger crossmodal (AV or VA) than unimodal connectivity in the control group.

[b]Stronger crossmodal (AV or VA) than unimodal connectivity in the PD group.

B = bilateral; BA = Brodmann area; GP = globus pallidus; IFG = inferior frontal gyrus; L = left; MTG = middle temporal gyrus; R = right; SFG = superior frontal gyrus; SMA = supplementary motor area.

Table 7.

Mean (standard deviation) striatal volumes[1] in the PD and control groups

	Control	PD	*t* value	*p*
Left caudate	0.244 (0.034)	0.228 (0.024)	1.96	0.056
Right caudate	0.252 (0.030)	0.234 (0.023)	2.43	0.019
Left putamen	0.374 (0.068)	0.337 (0.052)	2.23	0.031
Right putamen	0.360 (0.062)	0.323 (0.053)	2.28	0.027

[1]Volumes adjusted for total intracranial volume (eTIV).